Erratum: "Cysteine linkages accelerate electron flow through tetra-heme protein STC" [J. Am. Chem. Soc., vol. 139, pp. 17237–17240, 2017]

Xiuyun Jiang, Aldenek Futera, Ali, Ali, Fruzsina Gajdos, Guido F. von Rudorff, Antoine Carof, Marian Breuer, Jochen Blumberger Ali, Karan Breuer, Guido F. von Rudorff, Antoine Carof, Marian Breuer, Marian Breuer, Guido F. von Rudorff, Marian Breuer, Guido F. von Rudorff, Antoine Carof, Marian Breuer, Guido F. von Rudorff, Guido F. von Rudorff, Guido F. von Rudorff, Guido F. von Rudorff, Marian Breuer, Guido F. von Rudorff, Guido F. von

March 8, 2021

 ^a University College London, Department of Physics and Astronomy, Gower Street, London WC1E 6BT, UK
 ^b Institute for Advanced Study, Technische Universität München, Lichtenbergstrasse 2 a, D-85748 Garching,
 Germany

^{*} to whom correspondence should be addressed: e-mail: j.blumberger@ucl.ac.uk (J.B.)

We noted a mistake in our calculation of electronic coupling matrix elements between heme cofactors using the POD method. This resulted in a small change in the electron flux we reported for the tetraheme cytochrome STC. However, all conclusions of the original, published manuscript remain valid. In the following we give a detailed description of this error and amendments of main text, figures and tables.

In the POD/PBE50 calculations reported, the PBE exchange energy was scaled by 50% and, erroneously, not replaced by 50% HFX exchange. We have recently benchmarked again POD calculations against highlevel ab-initio calculations? add reference once paper is published and concluded that POD/PBE coupling values scaled by a factor of 1.394 gives excellent agreement with the high-level ab-initio data on the HAB11 database of pi-conjugated dimers? (mean relative unsigned error after scaling is 3.5%) Hence, we have recalculated the heme-heme electronic couplings in STC with POD/PBE and scaled the values obtained by a factor of 1.394. As in the original manuscript, the three highest lying minority spin orbitals on each heme are two d_{π} orbitals composed of Fe d_{xz} and d_{yz} and heme ring orbitals, denoted $d_{\pi,1}$ and $d_{\pi,2}$, respectively, and one $d_{||}$ orbital composed of Fe d_{xy} and heme ring orbital. The minority spin HOMO orbital on each heme is either $d_{\pi,1}$ or $d_{\pi,2}$, or a linear combination thereof, depending on the snapshot geometry. It is at least 0.1 eV above the minority spin HOMO-1 orbital in each snapshot. The $d_{||}$ orbital is always below the HOMO and either HOMO-1 or HOMO-2. As the energy spacing between HOMO and HOMO-1 is large compared to the thermal energy, it appears appropriate to consider the coupling between HOMO orbitals of donor and acceptor heme, only. However, the energy spacing between the d-orbitals is rather sensitive to the exchange correlation functional used. According to experimental EPR data the spin density of Fe³⁺-heme is described as originating from the Fe d_{xz} and Fe d_{yz} orbitals, which would suggest that both orbitals should be taken into account for coupling calculation. Hence, we report here two coupling values, the HOMO-HOMO coupling denoted "1 × 1", $|H_{ab}| = |\langle d_{\pi,i}^{A}|\bar{H}^{KS}|d_{\pi,j}^{D}\rangle|$, i = 1 or 2 (i.e., HOMO), and the coupling averaged over all 4 combinations of $d_{\pi,1}$ and $d_{\pi,2}$ orbitals on donor (D) and acceptor (A) hemes, denoted "2 × 2", $|H_{ab}| = [1/4 \sum_{i,j=1,2} |\langle d_{\pi,i}^{A} | \bar{H}^{KS} | d_{\pi,j}^{D} \rangle|^{2}]^{1/2}$.

We find that the two coupling protocols give similar result for the average coupling, i.e., for couplings averaged over the trajectory, see updated Table S2 below. Moreover, the difference with respect to the values reported in the original manuscript are reasonably small (max differences less than a factor of 2 **Sharon check**). Consequently, the electron transfer rates and fluxes calculated are also reasonably similar for the two methods (differences equal or less than factor of 2 for the final model **Sharon check**) and close to the originally reported values (difference equal or less than factor of 3 for final model **Sharon check**), see updated Table S4 and Figure 3. More specifically, using the 1×1 coupling protocol, the average coupling values for the final heme pair model changed by -21%, +29% and +45% for pairs 1-2, 2-3 and 3-4; as a result, the flux decreased by a factor of 1.1 and 1.5 for the $1 \to 4$ and $4 \to 1$ directions, respectively. Using the 2×2 coupling protocol, the average coupling values for the final model changed by -40%, -3% and -6% for the heme pairs 1-2, 2-3 and 3-4; as a result, the flux decreased by a factor of 2 and 3 for the $1 \to 4$ and $4 \to 1$ directions, respectively. We also noticed that while the 2×2 coupling values appear very robust with respect to the QM model chosen, the 1×1 coupling values are rather sensitive in this respect. Hence we generally recommend calculation of 2×2 couplings but note that 1×1 couplings can give good estimates when averaged over molecular dynamics trajectories.

In the following we summarize the amendments to the main text.

- line 21, "electron flux through STC in the thermodynamic downhill direction (heme $1 \to 4$) is $\approx 3 \times 10^6 \text{s}^{-1} (1 \times 1)/2 \times 10^6 \text{s}^{-1} (2 \times 2)$."
- line 24, "significantly enhanced the overall electron flow, by a factor of about 54 $(1 \times 1)/74$ (2×2) ."
- line 109, "a significant increase in electronic coupling by a factor of 7.3 $(1 \times 1)/3.3$ (2×2) ."
- line 111, "have only a minor effect for 2×2 ."

- line 113, "differs by less than 8% (2 × 2)."
- line 141, "a strong increase upon inclusion of cysteine linkages in the model is observed in all 2×2 calculations."
- line 149, "for heme pair 3-4 is a factor of 7.7 $(1 \times 1)/5.8$ (2×2) ."
- line 152, "for the other T-shaped heme pair 1-2, a factor of 7.4 $(1 \times 1)/8.7$ (2×2) , is even more pronounced"
- line 187, "an increase in the ET rate constants by a factor of 56 $(1 \times 1)/75$ (2×2) and 60 $(1 \times 1)/31(2 \times 2)$ to $3 \times 10^6 \mathrm{s}^{-1}$ $(1 \times 1)/2 \times 10^6 \mathrm{s}^{-1}$ (2×2) and $1 \times 10^7 \mathrm{s}^{-1}$ $(1 \times 1)/5 \times 10^6 \mathrm{s}^{-1}$ (2×2) for k_{21} and k_{43} , respectively"

 Sharon please change all 1x1 to 1×1 and similar for 2x2
- line 189, "significantly reducing the gap to the fastest ET rate between hemes 2-3, $k_{32} = 6 \times 10^8 \text{s}^{-1}$ $(1\text{x}1)/4 \times 10^8 \text{s}^{-1}$ (2x2)"
- line 235, "We obtain values of $3 \times 10^6 \mathrm{s}^{-1} \ (1\mathrm{x}1)/2 \times 10^6 \mathrm{s}^{-1} \ (2\mathrm{x}2)$ for the forward direction ... and $5 \times 10^5 \mathrm{s}^{-1} \ (1\mathrm{x}1)/3 \times 10^5 \mathrm{s}^{-1} \ (2\mathrm{x}2)$ for the reverse direction, corresponding to a flux enhancement of a factor of 54 $(1\mathrm{x}1)/74 \ (2\mathrm{x}2)$ and 52 $(1\mathrm{x}1)/72 \ (2\mathrm{x}2)$, respectively"
- Figure 2 updated, see below.
- Figure 3 updated, see below.

Figure 2: $|H_{ab}|$ values for heme pair 3-4. (A) Convergence with respect to the model size, as obtained with POD and FODFT methods for different DFT functionals. The sharp increase in coupling from 1 to 2 is due to inclusion of the cysteine linkages in model 2. The bold arrow indicates the final model chosen for presented rate calculations. (B) Thermal fluctuations of $|H_{ab}|$ at sPOD/PBE level along a MD trajectory using model 1 (green) and model 2 (blue). Dashed/Dotted lines indicate the accumulated average $\langle |H_{ab}|^2 \rangle^{\frac{1}{2}}$ for the large/small model.

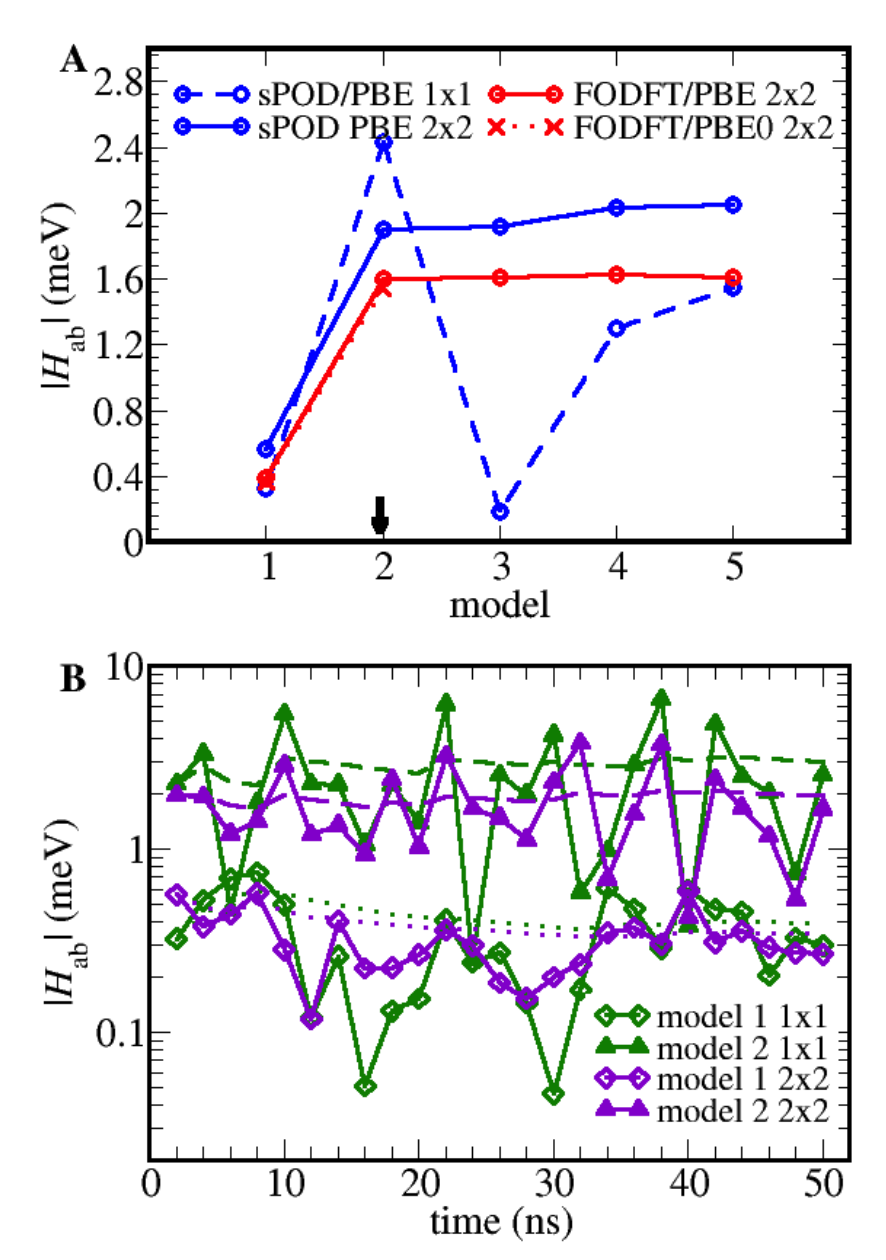
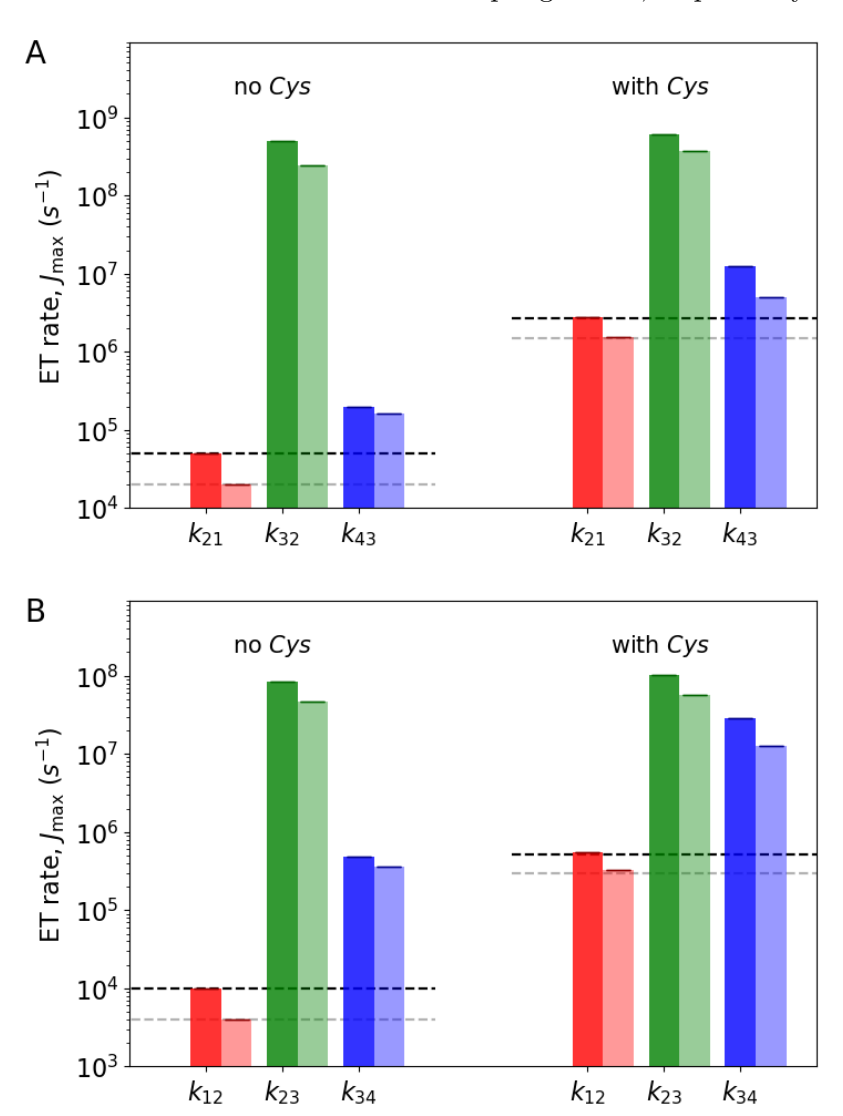


Figure 3: Heme-heme ET rate constants, k_{ji} , and the protein limited electron flux, J_{max} (dashed lines), for the steady-state electron flow in the forward direction from heme 1 to 4 (A) and in the reverse direction (B). The first set of bars in each panel was obtained for model 1, i.e. without cysteine linkages, the second sets included them (model 2, 3 for heme pairs 3-4, 1-2). MD-averaged coupling values at sPOD/PBE level of theory were used for calculation of the ET rates. Data taken from column "(SC,p)" in Table S4. Full and transparent bars are for 1×1 and 2×2 electronic coupling values, respectively.



In the following we summarize the amendments to the SI.

- Table S2. The updated values for coupling matrix elements using 1×1 and 2×2 averaging protocols.
- Table S4. The updated values for the maximum electron flux J_{max} , split into two tables, one for "1×1" and one for "2 × 2".
- Figure S3.
- Figure S5.

Table S2: Computed heme-heme electron transfer parameters for the STC protein. λ is the reorganization free energy obtained from MD simulation (see SI section 1.2), $\langle |H_{ij}|^2 \rangle^{1/2}$ is the average electronic coupling matrix element (see SI section 2.1 and 2.2). Models used are detailed in Table S1 and Figures S1-S2. In model 1 all heme ring substituents including the cysteine linkages are replaced by H, in the "final model" all relevant cysteine linkages are included. "Final model" refers to model 3 for heme pair 1-2, model 2 for pair 2-3 and model 2 for 3-4. All energies are given in meV.

| | | (- | $H_{ij} ^2\rangle^{1/2}$, mo | odel 1 | $\langle H_{ij} ^2 \rangle^{1/2}$, final model | | | |
|-----------------|---------------|-----------------|-------------------------------|-----------------|--|-----------------|-----------------|--|
| heme pair $i-j$ | λ | sPOD | /PBE | sFODFT/PBE | sPOD | /PBE | sFODFT/PBE | |
| | | 1×1 | 2×2 | 2×2 | 1×1 | 2×2 | 2×2 | |
| $\frac{1-2}{}$ | 1080 ± 80 | 0.23 ± 0.10 | 0.15 ± 0.02 | 0.31 ± 0.07 | 1.71 ± 0.23 | 1.31 ± 0.26 | 1.37 ± 0.25 | |
| 2 - 3 | 760 ± 50 | 3.55 ± 1.01 | 2.61 ± 0.59 | 3.30 ± 0.80 | 3.96 ± 0.89 | 2.99 ± 0.82 | 3.95 ± 1.08 | |
| $3\!-\!4$ | 880 ± 60 | 0.39 ± 0.16 | 0.34 ± 0.09 | 0.52 ± 0.05 | 3.02 ± 0.59 | 1.96 ± 0.41 | 2.11 ± 0.34 | |

Table S4 (1x1): Summary of electron flux calculations in STC. In the "final model" the ET rates k_{ji} are calculated with electronic coupling matrix elements obtained from models including the cysteine linkages and in model 1 without cysteine linkages. sPOD/PBE couplings and λ values from Table S2 are used. The protein limited steady-state fluxes, J_{max} , in the forward and reverse directions are calculated as described in SI sections 3.1 and 3.2. The reduction potentials used for calculations of J_{max} are indicated in parenthesis: (R,p): reduction potentials in all-reduced state, ionization center (IC) protonated, (SC,p): self-consistent iteration of reduction potentials with IC protonated, (R,d): reduction potentials of all-reduced state with IC deprotonated, (SC, d): self-consistent iteration of reduction potentials with IC deprotonated, (O,d): reduction potentials of all-oxidized state, ionization center (IC) deprotonated. The rate constants for ET from heme i to j, k_{ji} , and J_{max} are given in units of $10^6 \, \text{s}^{-1}$.

| | final model | | | | | | | | | | | |
|------------|------------------------|---------|-------|---------|-------|-------|--------------------------------|-------|---------|-------|--|--|
| | forward flux $1 \to 4$ | | | | | | reverse flux $4 \rightarrow 1$ | | | | | |
| | (R,p) | (SC, p) | (R,d) | (SC, d) | (O,d) | (R,p) | (SC, p) | (R,d) | (SC, d) | (O,d) | | |
| k_{21} | 2.2 | 2.8 | 2.1 | 3.0 | 5.3 | 2.2 | 3.6 | 2.1 | 3.5 | 5.3 | | |
| k_{32} | 344 | 607 | 223 | 333 | 275 | 344 | 321 | 223 | 199 | 275 | | |
| k_{43} | 45 | 12 | 107 | 34 | 28 | 45 | 35 | 107 | 85 | 28 | | |
| k_{12} | 0.96 | 0.74 | 1.00 | 0.67 | 0.36 | 0.96 | 0.56 | 1.00 | 0.56 | 0.36 | | |
| k_{23} | 96 | 50 | 152 | 99 | 122 | 96 | 103 | 152 | 170 | 122 | | |
| k_{34} | 22 | 78 | 8.6 | 29 | 36 | 22 | 29 | 8.6 | 11 | 36 | | |
| P_1 | 1.00 | 1.00 | 1.00 | 1.00 | 1.00 | 0.00 | 0.00 | 0.00 | 0.00 | 0.00 | | |
| P_2 | 0.02 | 0.03 | 0.02 | 0.04 | 0.10 | 0.87 | 0.94 | 0.86 | 0.94 | 0.98 | | |
| P_3 | 0.05 | 0.22 | 0.02 | 0.08 | 0.17 | 0.96 | 0.98 | 0.90 | 0.95 | 0.99 | | |
| P_4 | 0.00 | 0.00 | 0.00 | 0.00 | 0.00 | 1.00 | 1.00 | 1.00 | 1.00 | 1.00 | | |
| J_{\max} | 2.1 | 2.7 | 2.0 | 2.9 | 4.8 | 0.83 | 0.52 | 0.85 | 0.53 | 0.35 | | |

| | | | | | mod | lel 1 | | | | | | |
|--------------|------------------------|---------|-------|---------|-------|-------|--------------------------------|-------|---------|-------|--|--|
| | forward flux $1 \to 4$ | | | | | | reverse flux $4 \rightarrow 1$ | | | | | |
| | (R,p) | (SC, p) | (R,d) | (SC, d) | (O,d) | (R,p) | (SC, p) | (R,d) | (SC, d) | (O,d) | | |
| k_{21} | 0.04 | 0.05 | 0.04 | 0.05 | 0.10 | 0.04 | 0.06 | 0.04 | 0.06 | 0.10 | | |
| k_{32} | 277 | 502 | 180 | 274 | 221 | 277 | 258 | 180 | 160 | 221 | | |
| k_{43} | 0.75 | 0.20 | 1.8 | 0.56 | 0.47 | 0.75 | 0.58 | 1.8 | 1.4 | 0.47 | | |
| k_{12} | 0.02 | 0.01 | 0.02 | 0.01 | 0.01 | 0.02 | 0.01 | 0.02 | 0.01 | 0.01 | | |
| k_{23} | 77 | 39 | 122 | 78 | 98 | 77 | 83 | 122 | 137 | 98 | | |
| k_{34} | 0.37 | 1.3 | 0.14 | 0.50 | 0.59 | 0.37 | 0.48 | 0.14 | 0.19 | 0.59 | | |
| P_1 | 1.00 | 1.00 | 1.00 | 1.00 | 1.00 | 0.00 | 0.00 | 0.00 | 0.00 | 0.00 | | |
| P_2 | 0.02 | 0.02 | 0.01 | 0.03 | 0.09 | 0.87 | 0.94 | 0.85 | 0.94 | 0.98 | | |
| P_3 | 0.05 | 0.23 | 0.02 | 0.09 | 0.19 | 0.96 | 0.98 | 0.89 | 0.95 | 0.99 | | |
| P_4 | 0.00 | 0.00 | 0.00 | 0.00 | 0.00 | 1.00 | 1.00 | 1.00 | 1.00 | 1.00 | | |
| $J_{ m max}$ | 0.04 | 0.05 | 0.04 | 0.05 | 0.09 | 0.02 | 0.01 | 0.02 | 0.01 | 0.01 | | |

Table S4 (2x2).

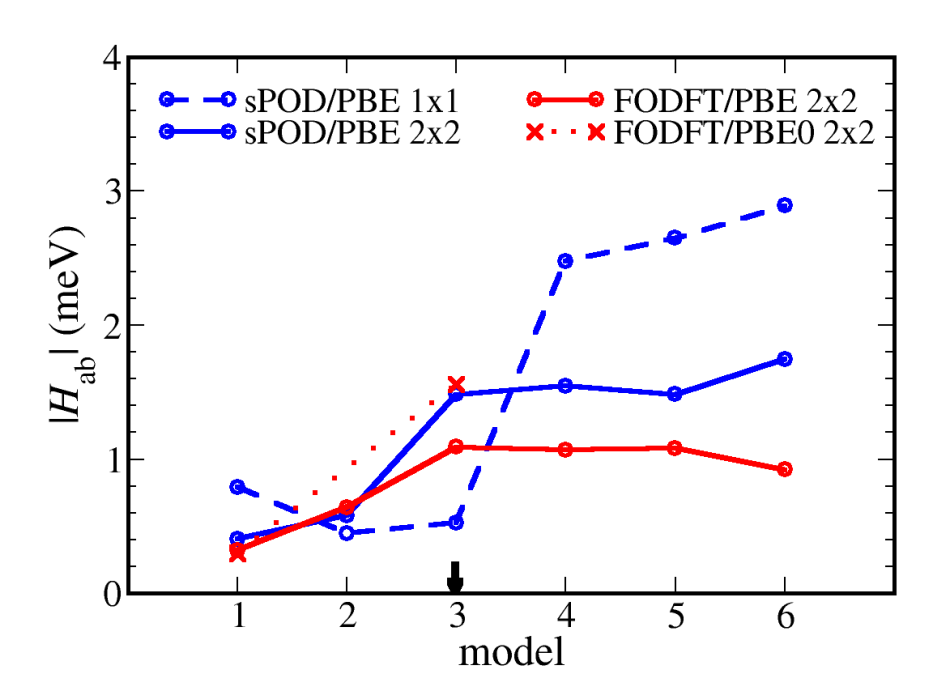
| c 1 | 1 1 |
|-------|-------|
| tinal | model |
| шиа | moder |

| | forward flux $1 \to 4$ | | | | | reverse flux $4 \to 1$ | | | | | |
|--------------|------------------------|---------|-------|---------|-------|------------------------|---------|-------|---------|-------|--|
| | (R,p) | (SC, p) | (R,d) | (SC, d) | (O,d) | (R,p) | (SC, p) | (R,d) | (SC, d) | (O,d) | |
| k_{21} | 1.3 | 1.5 | 1.2 | 1.7 | 3.1 | 1.3 | 2.1 | 1.2 | 2.1 | 3.1 | |
| k_{32} | 196 | 377 | 128 | 195 | 157 | 196 | 188 | 128 | 115 | 157 | |
| k_{43} | 19 | 5.0 | 45 | 14 | 12 | 19 | 14 | 45 | 36 | 12 | |
| k_{12} | 0.56 | 0.47 | 0.59 | 0.41 | 0.21 | 0.56 | 0.33 | 0.59 | 0.33 | 0.21 | |
| k_{23} | 55 | 26 | 87 | 55 | 70 | 55 | 58 | 87 | 97 | 70 | |
| k_{34} | 9.4 | 34 | 3.6 | 12 | 15 | 9.4 | 13 | 3.6 | 4.8 | 15 | |
| P_1 | 1.00 | 1.00 | 1.00 | 1.00 | 1.00 | 0.00 | 0.00 | 0.00 | 0.00 | 0.00 | |
| P_2 | 0.03 | 0.03 | 0.03 | 0.04 | 0.14 | 0.83 | 0.92 | 0.81 | 0.92 | 0.97 | |
| P_3 | 0.07 | 0.29 | 0.03 | 0.11 | 0.23 | 0.95 | 0.98 | 0.87 | 0.94 | 0.99 | |
| P_4 | 0.00 | 0.00 | 0.00 | 0.00 | 0.00 | 1.00 | 1.00 | 1.00 | 1.00 | 1.00 | |
| $J_{ m max}$ | 1.2 | 1.5 | 1.2 | 1.7 | 2.7 | 0.47 | 0.30 | 0.48 | 0.31 | 0.20 | |

| model | 1 |
|-------|---|
| model | |

| | model 1 | | | | | | | | | | | |
|--------------|------------------------|---------|-------|---------|-------|-------|--------------------------------|-------|---------|-------|--|--|
| | forward flux $1 \to 4$ | | | | | | reverse flux $4 \rightarrow 1$ | | | | | |
| | (R,p) | (SC, p) | (R,d) | (SC, d) | (O,d) | (R,p) | (SC, p) | (R,d) | (SC, d) | (O,d) | | |
| k_{21} | 0.02 | 0.02 | 0.02 | 0.02 | 0.04 | 0.02 | 0.03 | 0.02 | 0.03 | 0.04 | | |
| k_{32} | 150 | 243 | 97 | 143 | 120 | 150 | 136 | 97 | 86 | 120 | | |
| k_{43} | 0.57 | 0.16 | 1.4 | 0.43 | 0.36 | 0.57 | 0.46 | 1.4 | 1.1 | 0.36 | | |
| k_{12} | 0.01 | 0.01 | 0.01 | 0.01 | 0.003 | 0.01 | 0.004 | 0.01 | 0.004 | 0.003 | | |
| k_{23} | 42 | 24 | 66 | 44 | 53 | 42 | 46 | 66 | 75 | 53 | | |
| k_{34} | 0.29 | 0.96 | 0.11 | 0.38 | 0.45 | 0.29 | 0.36 | 0.11 | 0.14 | 0.45 | | |
| P_1 | 1.00 | 1.00 | 1.00 | 1.00 | 1.00 | 0.00 | 0.00 | 0.00 | 0.00 | 0.00 | | |
| P_2 | 0.01 | 0.02 | 0.01 | 0.02 | 0.05 | 0.92 | 0.97 | 0.91 | 0.97 | 0.99 | | |
| P_3 | 0.03 | 0.13 | 0.01 | 0.05 | 0.11 | 0.98 | 0.99 | 0.94 | 0.97 | 0.99 | | |
| P_4 | 0.00 | 0.00 | 0.00 | 0.00 | 0.00 | 1.00 | 1.00 | 1.00 | 1.00 | 1.00 | | |
| $J_{ m max}$ | 0.02 | 0.02 | 0.02 | 0.02 | 0.04 | 0.01 | 0.004 | 0.01 | 0.004 | 0.003 | | |

Figure S3: Electronic coupling matrix elements $|H_{ab}|$ for the computational models defined in Table S1 and Figures S1-S2, for heme pair 1-2 (upper panel) and 2-3 (lower panel). Results for heme pair 3-4 have been shown in the main text.



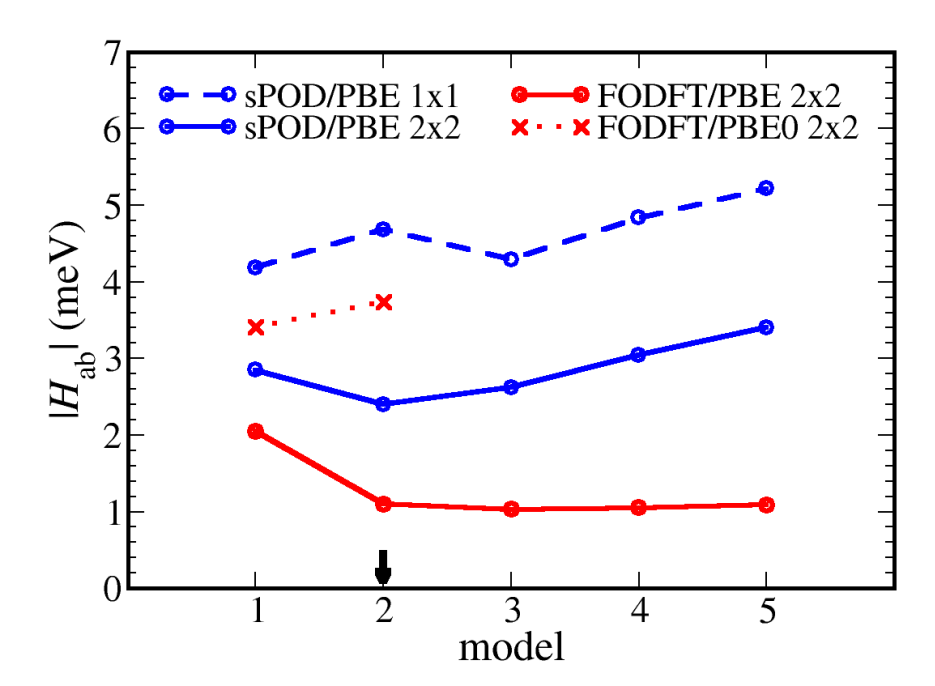


Figure S5: Thermal fluctuations of electron coupling matrix elements calculated with POD/PBE50 along the MD trajectories for heme pair 1-2 (upper panel) and 2-3 (lower panel), for model 1 (green, no cysteine linkages) and the respective final models in blue, model 3 for heme pair 1-2 (with cysteine linkages), and model 2 for 2-3. Dash/Dotted lines indicate the accumulated average $\langle |H_{\rm ab}^2| \rangle^{1/2}$ for the large/small model. Results for heme pair 3-4 have been shown in the main text.

